Pion electronic decay and lepton universality

D. Počanić[1*], for the PEN Collaboration

1 University of Virginia, Charlottesville, VA 22904-4714, USA
* pocanic@virginia.edu

11 May 2021

Abstract

In common with a number of simple processes involving elementary particles, charged pion decays are profoundly shaped by applicable Standard Model (SM) symmetries and properties. Given the highly precise SM theoretical description, pion decays are used as selective probes of SM parameters, and of possible SM extensions. The PEN experiment at PSI is studying the $\pi^+ \to e^+ \nu_e(\gamma)$, or $\pi_{e2(\gamma)}$ decay. The primary goal is to reach the relative precision of 5×10^{-4} in $R^\pi_{e/\mu}$, the branching ratio for $\pi_{e2(\gamma)}$ decay. We review the PEN research program, its present status, and prospects.

25.1   Motivation

Immediately following the discovery of the charged pion, its decays presented a puzzle: absence of the direct pion decay to an electron that persisted for over a decade. The solution to the puzzle became prominent among the early arguments for the $V-A$ form of the "universal" weak interaction [1]. The $V-A$ helicity suppression of the right-handed state of the electron led to the accurate prediction [2] of the tree level $\pi \to e\bar{\nu}(\gamma)$, or $\pi_{e2(\gamma)}$[1] branching fraction, $R^\pi_{e/\mu,0}$, even before the decay itself was discovered [3]:

$$R^\pi_{e/\mu,0} \equiv \frac{\Gamma(\pi \to e\bar{\nu})}{\Gamma(\pi \to \mu\bar{\nu})} = \frac{m_e^2}{m_\mu^2} \cdot \frac{(m_\pi^2 - m_e^2)^2}{(m_\pi^2 - m_\mu^2)^2} \simeq 1.283 \times 10^{-4}. \tag{25.1}$$

In the years that followed, π_{e2} decay served as an important theory testing ground, providing rapid experimental confirmations [4,5] for predicted radiative corrections [6,7]. This close interplay with theory, at the edge of experimentally accessible precision, remains the driving force behind π_{e2} measurements today.

In terms of its underlying physics, the π_{e2} decay stands out. By comparison, the much rarer $\mathcal{O}(10^{-8})$ pion beta, $\pi^+ \to \pi^0 e^+ \nu$, or π_{e3}, decay is fully allowed in the SM. It is suppressed only by the small available final-state phase space: a major hindrance to experimental study of an otherwise ultra clean SM process. On the other hand, the strong helicity suppression of the π_{e2} decay (squared lepton mass ratio in Eq. (25.1)) makes this decay uniquely sensitive to a class of pseudoscalar[2] (P), or P-loop-coupled, non-($V-A$) contributions, arising from new, "beyond Standard Model" (BSM) physics, undetectable in analogous, helicity-unsuppressed leptonic decays, such as the $\pi \to \mu\bar{\nu}$, or $\pi_{\mu2}$.

---

[1]A γ in parentheses denotes an undetected, usually soft photon. For brevity, in further text the (γ) will be dropped and implied; a detected photon in radiative processes will be explicitly denoted with a γ.

[2]The $\pi^- \to \ell\bar{\nu}_\ell$ decay connects the pion pseudoscalar 0^- state to the 0^+ vacuum.

34 A more complete treatment of π_{e2} includes $\delta R^{\pi}_{e/\mu}$, the radiative and loop corrections, and
35 the possibility of lepton universality (LU) violation, i.e., that g_e and g_μ, the electron and muon
36 W couplings, may not be equal:

$$R^{\pi}_{e/\mu} \equiv \frac{\Gamma(\pi \to e\,\bar{\nu}(\gamma))}{\Gamma(\pi \to \mu\,\bar{\nu}(\gamma))} = \frac{g_e^2}{g_\mu^2} \frac{m_e^2}{m_\mu^2} \frac{(m_\pi^2 - m_e^2)^2}{(m_\pi^2 - m_\mu^2)^2} \left(1 + \delta R^{\pi}_{e/\mu}\right). \tag{25.2}$$

37 Steady improvements of the SM description of the π_{e2} decay have reached the precision
38 level of 8 parts in 10^5: $R^{\pi,\mathrm{SM}}_{e/\mu} = 1.2352(1) \times 10^{-4}$ [8–10], which indicates that the radia-
39 tive and loop corrections amount to ~4% of $R^{\pi}_{e/\mu}$. The best current experimental result,
40 $R^{\pi,\mathrm{exp}}_{e/\mu} = 1.2327(23) \times 10^{-4}$, dominated by measurements at TRIUMF and PSI [11–14], is
41 23 times less precise than the theoretical one.
42 The primary motivation for the PEN [15] experiment is the unique sensitivity of the π_{e2} de-
43 cay to BSM processes is. The international PEN collaboration, led by the University of Virginia
44 (UVa) group, set out to measure $R^{\pi}_{e/\mu}$ at PSI, with a relative precision of $\Delta R^{\pi}_{e/\mu}/R^{\pi}_{e/\mu} \le 5 \times 10^{-4}$.
45 At $\Delta R/R = 10^{-3}$, π_{e2} probes the pseudoscalar and axial vector mass scales up to 1,000 TeV
46 and 20 TeV, respectively [16, 17]. For comparison, unitarity tests of the Cabibbo-Kobayashi-
47 Maskawa matrix and precise measurements of superallowed nuclear beta decays constrain
48 the non-SM vector contributions to > 20 TeV, and scalar ones to > 10 TeV [14]. Although
49 scalar interactions do not directly contribute to $R^{\pi}_{e/\mu}$, they can do so through loop diagrams,
50 resulting in a sensitivity to new scalar interactions up to 60 TeV [16, 17]. The subject was
51 recently reviewed in Refs. [18, 19]. In addition, $R^{\pi,\mathrm{exp}}_{e/\mu}$ provides limits on the masses of certain
52 SUSY partners [20], and on anomalies in the neutrino sector [21]. Mounting indications [22]
53 of LU violation in B-meson decays make the subject additionally interesting (for a review see,
54 e.g., [23]).
55 Additional goals of PEN include measurements of the radiative $\pi_{e2\gamma}$, and $\mu^+ \to e^+ \nu \bar{\nu} \gamma$
56 decays, as well as of τ_{π^+}, the pion mean life. The physics motivation for the study of $\pi_{e2\gamma}$
57 decay is discussed in [24], in the context of the PiBeta experiment, predecessor to PEN. Muon
58 decays, sensitive to non-$(V-A)$ contributions, are not discussed here; neither is τ_{π^+}.

25.2 The PEN apparatus

60 As the successor to the PiBeta experiment, PEN took over the major components of this appa-
61 ratus [24, 25], with enhancements and upgrades. PEN detected and analyzed decays of pions
62 and muons at rest in this detector. The 240-element pure CsI crystal calorimeter and the two
63 multiwire proportional chambers (MWPC1,2) were serviced but otherwise unmodified. The
64 3.2 mm thick plastic hodoscope (PH) array, exhibiting surface crazing, was rebuilt with new
65 fast 4 mm thick plastic scintillator staves. The central beam detectors were reconfigured, as
66 seen in Figure 25.1. The upstream beam counter (BC) was rebuilt, the beam vacuum pipe
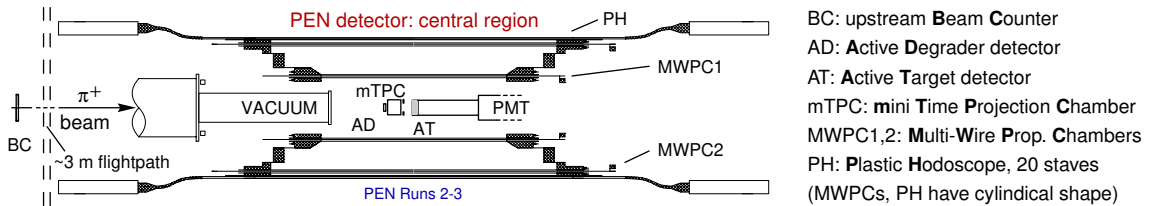
Figure 25.1: Schematic drawing of the central detector region in the PEN Runs 2–3
configuration, including the mTPC for beam tracking (see text for further details).

67 was extended closer to the redesigned active degrader (AD) and the new one-piece active tar-
68 get (AT); all were optimized for the lower beam momentum $p_\pi \simeq 75\,\text{MeV}/c^2$, compared to
69 $\simeq 114\,\text{MeV}/c^2$ in PiBeta running. The addition of PEN beam tracking detectors, discussed be-
70 low, was also important. Three data-acquisition runs were completed from 2008 through 2010
71 in the PSI πE1 beam area. Over $\sim$25 weeks of beam, PEN accumulated $N_{\pi \to e\nu} \simeq 2.3 \times 10^7$,
72 and $N_{\pi \to \mu \to e} > 1.5 \times 10^8$ events, along with significant numbers of pion and muon radiative
73 decays.

74 During PEN Run 1, a plastic scintillator degrader made of four slanted wedges, was used
75 for beam tracking. The wedge tracker was replaced in Runs 2 and 3 with low-mass mini time
76 projection chambers, mTPCs, which improved the spatial resolution. The mTPCs, their design,
77 performance, and the key input they provide in the analysis, are described in [26]. Signals
78 from the beam detectors were sent to waveform digitizers, running at 2 GS/s for BC, AD, and
79 AT, and at 250 MS/s for the mTPC. Given the critical role of the mTPCs in controlling the $R^\pi_{e/\mu}$
80 systematics, the analysis reported here excludes Run 1, or $\sim$20% of the full PEN data set.

81 **25.3 Pion electronic decay: $\pi^+ \to e^+ \nu_e(\gamma)$**

82 A long list of physical processes challenge any precise measurement of $R^\pi_{e/\mu}$ at rest, each com-
83 plicating the prime objective to accurately identify, sort, count, and normalize the recorded
84 π_{e2} and $\pi_{\mu2}$ decay events. It is a particular challenge to accurately separate and count the
85 π_{e2} events that fall in the "tail" of the calorimeter energy response, under the vastly more
86 numerous $\pi \to \mu \to e$ events. A number of observables are used to discriminate to some de-
87 gree between the π_{e2} and $\pi_{\mu2}$ decay events in the data. The most effective is "$\Delta\chi^2$" which
88 tests a filtered AT waveform [19] for agreement with 2-peak (π_{e2}), and 3-peak ($\pi_{\mu2}$) hypothe-
89 ses based on predicted π^+ and e^+ signals (Figure 25.2). Key to the effectiveness of the $\Delta\chi^2$
90 test are the (a) precise prediction of the decay vertex, based on the beam π^+ and decay e^+
91 tracking information, plus BC-AD time of flight, and (b) accurate calibration of the AT wave-
92 form [19, 26].

93 The effectiveness of the $\Delta\chi^2$ discriminator is highlighted in Figure 25.3, which shows
94 the separation of the π_{e2}, and $\pi_{\mu2}$ decays in the data. After subtraction of backgrounds, the
95 best experimental determination of the low-E response "tail" for π_{e2} events falls short of the
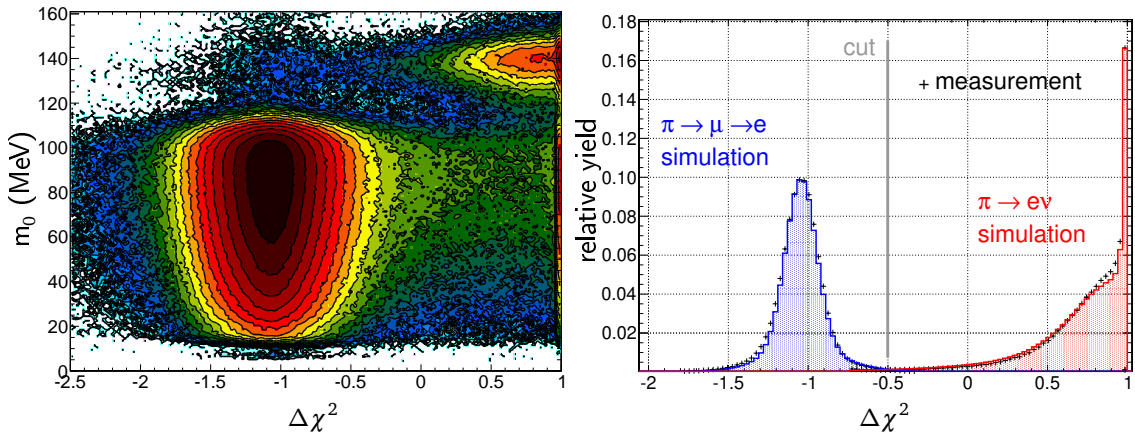
Figure 25.2: Separation of π_{e2} and $\pi_{\mu2}$ events through use of the $\Delta\chi^2$ observ-
able. Left: event invariant mass, $m_0^{e\nu/e\nu\gamma} = \sum E_i + |\sum \vec{p}_i|$, where i denotes distinct
tracks/showers and $c \equiv 1$, vs. $\Delta\chi^2$, for a set of Run 2 data recorded with a dedicated
$\pi_{\mu2}$-suppressed trigger. Right: $\Delta\chi^2$ distribution for a set of standard-trigger Run 2
events. Gray line: typical choice for the cut separating the two decay types.
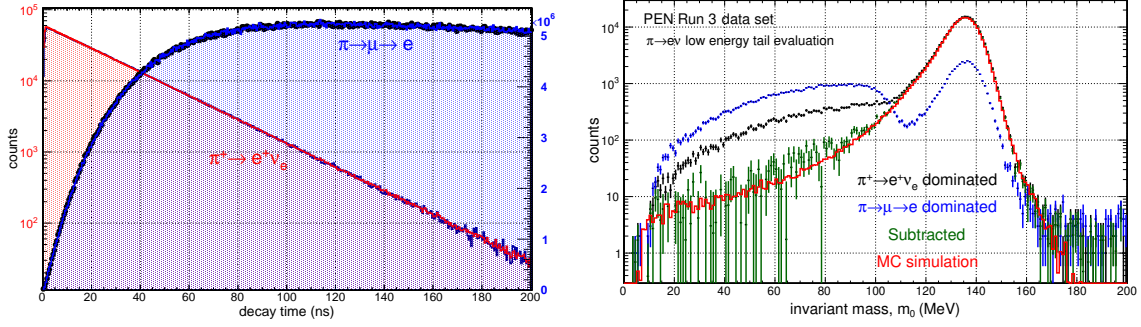
Figure 25.3: Left: decay time spectra for a subset of PEN Run 3 data (black crosses) with applied $\Delta\chi^2$ cuts shown in Figure 25.2. Geant4 simulation results are overlaid in red, for π_{e2}, and blue, for $\pi_{\mu2}$ decays. Right: low energy tail of the π_{e2} invariant mass, m_0, response before and after background subtraction for a subset of Run 3 data.

required precision, leaving the determination of the final factor of 5 in precision (Table 25.1) to Monte Carlo simulations. This goal was recently made possible with the inclusion of corrected photoneutron cross sections (γ, n) and $(\gamma, 2n)$ on ^{133}Cs and ^{127}I [26, 27] into Geant4.

The experimental branching ratio $R_{e/\mu}^{\pi,\mathrm{exp}}$ is determined as

$$R_{e/\mu}^{\pi,\mathrm{exp}} = \frac{N_{\pi\to e\nu}^{\mathrm{peak}}(1+\epsilon_{\mathrm{tail}})}{N_{\pi\to\mu\nu}} \cdot \frac{f_{\pi\to\mu\to e}(T_e)}{f_{\pi\to e\nu}(T_e)} \cdot \frac{\epsilon(E_{\mu\to e\nu\bar\nu})_{\mathrm{MWPC}}}{\epsilon(E_{\pi\to e\nu})_{\mathrm{MWPC}}} \cdot \frac{A_{\pi\to\mu\to e}}{A_{\pi\to e\nu}} \cdot \frac{\epsilon_{\mathrm{pileup}}}{\epsilon_{\delta\chi^2}} \tag{25.3}$$

$$= \frac{N_{\pi\to e\nu}^{\mathrm{peak}}}{N_{\pi\to\mu\nu}} \cdot (1+\epsilon_{\mathrm{tail}}) \cdot r_f \cdot r_{\mathrm{PC}} \cdot r_A \cdot r_{\mathrm{cut}}, \tag{25.4}$$

where ϵ_{tail} is the low energy tail fraction of the π_{e2} response, r_f is the ratio of the decay

Type	Observable	Value	$\Delta R_{e/\mu}^{\pi}/R_{e/\mu}^{\pi}$
Systematic:	$\Delta\epsilon_{\mathrm{tail}}$: low-$E$ "tail" fraction*	$\simeq 0.038$	$\begin{cases} \simeq 0.001^{\mathrm{exp}} \\ 2\times10^{-4}\vert_{\mathrm{goal}}^{\mathrm{MC}} \end{cases}$
	r_f: observed decay fractions	0.0441	$< 10^{-4}$
	r_{PC}: ratio of MWPC efficiencies	$\simeq .99$	$< 10^{-4}$
	r_A: acceptance ratio (blinded)	$\simeq 1$	$\leq 10^{-4}$
	r_{cut}: cut efficiency ratio	$\simeq 1.0153$	$\leq 4\times10^{-4}$
	$N_{\pi_{\mathrm{DIF}}\to e\nu}/N_{\pi\to e\nu}$	$< 2\times10^{-3}$	$10^{-6}-10^{-5}$
	$N_{\pi_{\mathrm{DIF}}\to\mu\nu}/N_{\pi\to\mu\nu}$	2.3×10^{-3}	$10^{-6}-10^{-5}$
	$N_{\mu_{\mathrm{DIF}}\to e\nu\bar\nu}/N_{\mu\to\nu\bar\nu}$	1.4×10^{-4}	$< 10^{-5}$
Statistical:	$\Delta N_{\pi\to e\nu}/N_{\pi\to e\nu}$		$\simeq 3\times10^{-4}$
Overall	goal		5×10^{-4}

* Depends on the chosen invariant mass cutoff, here $m_0 = 117.5$ MeV, which minimizes overall uncertainty.

Table 25.1: Projected uncertainty budget for the determination of $R_{e/\mu}^{\pi}$ in PEN, focusing on the dominant sources. Label "DIF" denotes decay in flight of the particle so marked.

101   fractions for the two processes within the observed decay time gates, r_{PC} is the ratio of the
102   MWPC efficiencies for the two processes, and r_A is the ratio of the geometrical acceptances for
103   the two processes, evaluated from simulation. The quantities needed to determine $R^\pi_{e/\mu}$, given
104   in (25.4), along with their uncertainties, are summarized in Table 25.1. As of this writing, a
105   final critical pass through the calibration and analysis parameters is underway, so that some
106   of the entries in the table may be improved.

25.4   Pion radiative electronic decay: $\pi^+ \rightarrow e^+ \nu_e \gamma$

108   The motivation for the measurement of the pion radiative electronic decay, $\pi_{e2\gamma}$, and results
109   obtained for this channel by the PiBeta collaboration are discussed in detail in [19, 24, 28].
110   Thanks to a more open trigger, new PEN data greatly extend the phase space coverage of the
111   $\pi_{e2\gamma}$ decay compared to PiBeta, of interst for determining the poorly known [28] amplitude
    $SD^- \propto (F_A - F_V)^2$. The region of peak sensitivity to SD^-, shown in Figure 25.4, is fully covered
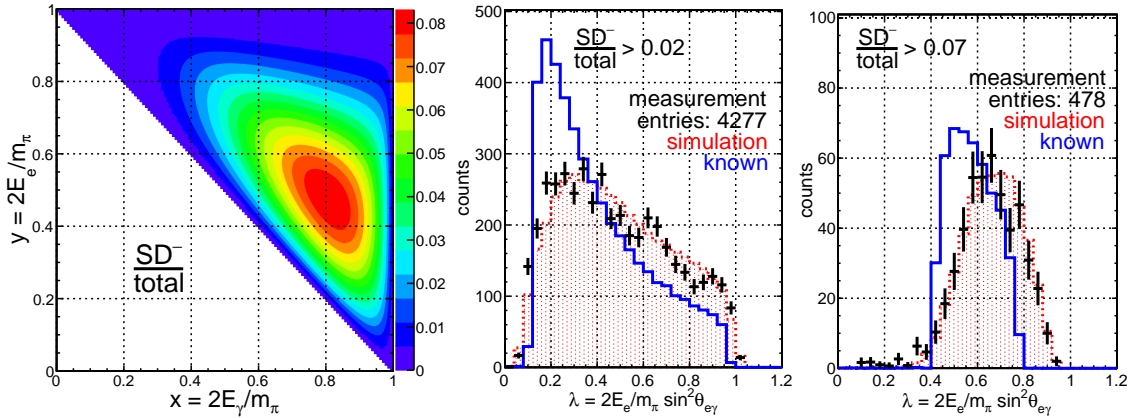
Figure 25.4: Left: phase space contours of constant fraction of the SD^- term in the
overall $\pi_{e2\gamma}$ differential decay rate, calculated using $F_{A,V}$ values after [28]. Center
and right: measured distributions (black) in λ for $SD^-/$total > 0.02 and 0.07, re-
spectively, compared with Geant4 "known" values at decay event creation (blue), and
results of realistic Geant4 simulation including the full effects of detector response
resolution (red).

113   in PEN for the first time. The other two panels in Figure 25.4 compare the measured data
114   and simulation using the best $F_{A,V}$ values of [28], updated in [19]. Expectations for a major
115   breakthrough in SD^- precision are tempered, however, by the low peak SD^- contribution
116   ($<10\%$) to the differential decay rate.

25.5   Conclusions

118   The PEN collaboration is on course to improve the experimental precision of the pion electronic
119   decay $\pi^+ \rightarrow e^+ \nu_e(\gamma)$ to a relative precision of $\sim 5 \times 10^{-4}$. In parallel with the current, final
120   round of analysis parameter tuning, the collaboration is preparing for publication a series of
121   technical papers describing the analysis, the first of which is [26]. Once the analysis is frozen,
122   the collaboration will unblind the main result for $R^\pi_{e/\mu}$. Integral to this program are the studies
123   of radiative pion ($\pi_{e2\gamma}$) and muon decays, as well as a new determination of τ_{π^+}, the charged
124   pion mean life.

Acknowledgments

This work has been supported by the U.S. National Science Foundation, the Paul Scherrer Institute, and the Russian Foundation for Basic Research.

References

[1] M. Ruderman and R. Finkelstein, *Note on the decay of the π-meson*, Phys. Rev. **76**(10), 1458 (1949), doi:10.1103/PhysRev.76.1458.

[2] R. P. Feynman and M. Gell-Mann, *Theory of Fermi interaction*, Phys. Rev. **109**, 193 (1958), doi:10.1103/PhysRev.109.193.

[3] T. Fazzini *et al.*, *Electron decay of the pion*, Phys. Rev. Lett. **1**, 247 (1958), doi:10.1103/PhysRevLett.1.247.

[4] H. L. Anderson, T. Fujii and R. H. Miller, *Branching ratio of the electronic mode of positive pion decay*, Phys. Rev. **119**, 2050 (1960), doi:10.1103/PhysRev.119.2050.

[5] E. Di Capua *et al.*, *Study of the decay $\pi \to e\nu$*, Phys. Rev. **133**, B1333 (1964), doi:10.1103/PhysRev.133.B1333.

[6] S. M. Berman, *Radiative corrections to pion β decay*, Phys. Rev. Lett. **1**, 468 (1958), doi:10.1103/PhysRevLett.1.468.

[7] T. Kinoshita, *Radiative corrections to π-e decay*, Phys. Rev. Lett. **2**, 477 (1959), doi:10.1103/PhysRevLett.2.477.

[8] W. J. Marciano and A. Sirlin, *Radiative corrections to π_{l2} decays*, Phys. Rev. Lett. **71**, 3629 (1993), doi:10.1103/PhysRevLett.71.3629.

[9] M. Finkemeier, *Radiative corrections to π_{l2} and K_{l2} decays*, Phys. Lett. B **387**, 391 (1996), doi:10.1016/0370-2693(96)01030-1, hep-ph/9505434.

[10] V. Cirigliano and I. Rosell, *Two-loop effective theory analysis of $\pi(K) \to e\bar{\nu}_e(\gamma)$ branching ratios*, Phys. Rev. Lett. **99**, 231801 (2007), doi:10.1103/PhysRevLett.99.231801, 0707.3439.

[11] D. I. Britton *et al.*, *Measurement of the pi+ —> e+ neutrino branching ratio*, Phys. Rev. Lett. **68**, 3000 (1992), doi:10.1103/PhysRevLett.68.3000.

[12] G. Czapek *et al.*, *Branching ratio for the rare pion decay into positron and neutrino*, Phys. Rev. Lett. **70**, 17 (1993), doi:10.1103/PhysRevLett.70.17.

[13] A. Aguilar-Arevalo *et al.*, *Improved measurement of the $\pi \to e\nu$ branching ratio*, Phys. Rev. Lett. **115**(7), 071801 (2015), doi:10.1103/PhysRevLett.115.071801, 1506.05845.

[14] P. Zyla *et al.*, *Review of Particle Physics*, PTEP **2020**(8), 083C01 (2020), doi:10.1093/ptep/ptaa104.

[15] *Pen experiment home page*, http://pen.phys.virginia.edu.

[16] B. A. Campbell and D. W. Maybury, *Constraints on scalar couplings from $\pi^{\pm} \to l^{\pm}\nu_l$*, Nucl. Phys. B **709**, 419 (2005), doi:10.1016/j.nuclphysb.2004.12.015, hep-ph/0303046.

[17] B. Campbell and A. Ismail, *Leptonic pion decay and physics beyond the electroweak Standard Model*, https://arxiv.org/abs/0810.4918 (2008), 0810.4918.

[18] D. Bryman, P. Depommier and C. Leroy, $\pi \rightarrow e\nu$, $\pi \rightarrow e\nu\gamma$ *decays and related processes*, Phys. Rept. **88**, 151 (1982), doi:10.1016/0370-1573(82)90162-4.

[19] D. Počanić, E. Frlež and A. van der Schaaf, *Experimental study of rare charged pion decays*, J. Phys. G **41**, 114002 (2014), doi:10.1088/0954-3899/41/11/114002, 1407.2865.

[20] M. Ramsey-Musolf, S. Su and S. Tulin, *Pion leptonic decays and supersymmetry*, Phys. Rev. D **76**, 095017 (2007), doi:10.1103/PhysRevD.76.095017, 0705.0028.

[21] W. Loinaz *et al.*, *The NuTeV anomaly, lepton universality, and nonuniversal neutrino gauge couplings*, Phys. Rev. D **70**, 113004 (2004), doi:10.1103/PhysRevD.70.113004, hep-ph/0403306.

[22] L. C. R. Aaij *et al.*, *Test of lepton universality in beauty-quark decays*, https://arxiv.org/abs/2103.11769 (2021), 2103.11769.

[23] G. Ciezarek *et al.*, *A challenge to lepton universality in B meson decays*, Nature **546**, 227 (2017), doi:10.1038/nature22346, 1703.01766.

[24] D. Počanić, *The pion beta and radiative electronic decays*, this volume of SciPost Phys. Proc.,paper 024 (2021).

[25] E. Frlež *et al.*, *Design, commissioning and performance of the PIBETA detector at PSI*, Nucl. Instrum. Meth. A **526**, 300 (2004), doi:10.1016/j.nima.2004.03.137, hep-ex/0312017.

[26] C. Glaser *et al.*, *Beam particle tracking with a low-mass mini time projection chamber in the PEN experiment*, https://arxiv.org/abs/2012.12266 (2020), 2012.12266.

[27] C. Glaser, D. Počanić and V. Baranov, *Monte Carlo simulation of the* (γ, n) *and* $(\gamma, 2n)$ *reactions on cesium and iodine below 100 MeV*, (in preparation) (2021).

[28] M. Bychkov *et al.*, *New precise measurement of the pion weak form factors in* $\pi^+ \rightarrow e^+ \nu\gamma$ *decay*, Phys. Rev. Lett. **103**, 051802 (2009), doi:10.1103/PhysRevLett.103.051802, 0804.1815.